

SLAM Mapping Method of Laser Radar for Tobacco Production Line Inspection Robot Based on Improved RBPF

Zhiyuan Liang, Pengtao He, Wenbin Liang, Xiaolei Zhao*, Bin Wei

Liuzhou Cigarette Factory, China Tobacco Guangxi Industrial Co., Ltd., Liuzhou, Guangxi, 545005, China

Abstract—The study focuses on the laser radar SLAM mapping method employed by the tobacco production line inspection robot, utilizing an enhanced RBPF approach. It involves the construction of a well-structured two-dimensional map of the inspection environment for the tobacco production line inspection robot. This construction aims to ensure the seamless execution of inspection tasks along the tobacco production line. The fusion of wheel odometer and IMU data is accomplished using the extended Kalman filter algorithm, wherein the resulting fused odometer motion model and LiDAR observation model jointly serve as the hybrid proposal distribution. In the hybrid proposal distribution, the iterative nearest point method is used to find the sampling particles in the high probability area, and the matching score during particle matching scanning is used as the fitness value, and the Drosophila optimization strategy is used to adjust the particle distribution. Then, the weight of each particle after optimization is solved, and the particles are adaptively resampled according to the size of the weight after solution, and the inspection map of the inspection robot of the tobacco production line is updated according to the updated position and posture information and observation information of the particles of the inspection robot of the tobacco production line. The experimental results show that this method can realize the laser radar SLAM mapping of the tobacco production line inspection robot, and it can build a more ideal two-dimensional map of the inspection environment of the tobacco production line inspection robot with fewer particles. If it is applied to practical work, a more ideal work effect can be achieved.

Keywords—Improved RBPF; tobacco production line; patrol robot; LiDAR; slam mapping; drosophila optimization strategy

I. INTRODUCTION

The inspection robot of tobacco production line can replace manual work to realize remote routine inspection [1]. In case of accidents and special circumstances, it can realize special inspection and customized inspection tasks, and realize remote online monitoring [2]. While reducing manual work, it can greatly improve the content and frequency of operation and maintenance, change the operation and maintenance mode of traditional tobacco production line, realize the intelligent operation and maintenance of tobacco production line, and greatly promote the development of tobacco enterprises [3]. Simultaneous Localization and Mapping (SLAM) technology has always been considered as the most critical step in achieving fully autonomous navigation of robots [4]. As a basic problem of tobacco production line patrol robots, laser

radar SLAM mapping is a prerequisite for tobacco production line patrol robots to achieve other functions. Whether the laser radar SLAM mapping of the tobacco production line patrol robot can be achieved well or not, to a large extent, determines whether the tobacco production line patrol can be successfully completed [5]. Therefore, it is very necessary to study an effective laser radar SLAM mapping method of the tobacco production line patrol robot to help the tobacco production line patrol work. Tobacco production line inspection robots need to obtain real-time environmental information and accurately locate themselves in the production line to effectively perform tasks. The LiDAR SLAM mapping method can realize simultaneous localization and map construction, so it is an ideal choice for tobacco production line inspection robots.

In response to the above problems, many scholars have carried out a lot of effective research, such as the map centered SLAM mapping method of intensive 3D laser anti-radar for tobacco production line patrol robots proposed by Park et al. [6], the active SLAM new method of tobacco production line patrol robots using laser radar to draw maps proposed by Malobick et al. [7], low delay laser radar SLAM for tobacco production line patrol robot using continuous scanning slices proposed by Karimi et al. [8], active SLAM method for tobacco production line patrol robot based on convolutional neural network proposed by Bol et al. [9], SLAM method for tobacco production line patrol robot based on embedded system on chip 3D positioning and mapping researched by Gerlein et al. [10]. Park et al., in their research on the laser radar SLAM mapping method of the tobacco production line inspection robot, took the map as the center, overcome the shortcomings such as the laser radar motion distortion through the local continuous time trajectory, and used the surface resolution maintenance matching algorithm and the surface fusion model based on the normal inverse Wisart to achieve non redundant but dense mapping. The traditional map centered laser radar SLAM method of tobacco production line inspection robot is improved. On the basis of realizing the laser radar SLAM mapping of tobacco production line inspection robot, the accuracy of laser radar SLAM mapping is significantly improved. Malobick et al. used the laser radar as the main sensor in their research on the laser radar SLAM mapping method of the tobacco production line inspection robot. After mapping the inspection environment of the tobacco production line inspection robot, they created a corresponding grid map to navigate the tobacco production line inspection robot system. In Karimi et al.'s research on the laser

radar SLAM mapping method of the tobacco production line inspection robot, 2D Lisaru rotation mode was used to drive the laser radar mounted on the tobacco production line inspection robot, and slice point cloud data from the rotating laser radar was used in the multithreaded matching pipeline for 6D attitude estimation with high update rate and low delay. At the same time, the attitude estimation uses the time motion predictor to better find the feature correspondence in the mapping. The experimental nonlinear optimizer converges quickly, and then completes the attitude fusion operation by using the extended Kalman filter algorithm. Finally, the robot patrol map is updated according to the obtained position and attitude and observation values; In the research of the laser radar SLAM mapping method of the tobacco production line inspection robot by Bol et al., a data set composed of environmental images and the wheel angles related to these environmental images is used to train the convolutional neural network structure so that the convolutional neural network model can learn how to guide the tobacco production line inspection robot. Then, in the inspection environment of tobacco production line inspection robot, it can navigate autonomously through convolutional neural network and obtain corresponding maps at the same time. Gerlein et al. followed a joint design method in their research on the laser radar SLAM mapping method of the tobacco production line inspection robot. By deploying a programmable 3D positioning and mapping chip in the tobacco production line patrol robot system, the laser radar SLAM of the tobacco production line patrol robot is realized, which effectively improves the SLAM mapping efficiency while maintaining a high mapping accuracy. The above methods can realize the laser radar SLAM mapping of tobacco production line inspection robot, but the mapping effect is not ideal.

The improved RBPF (Rao Blackwelled particle filter) is applied to the laser radar SLAM mapping of the tobacco production line inspection robot, which can yield more ideal results of the laser radar SLAM mapping of the tobacco production line inspection robot. Therefore, this paper proposes a laser radar SLAM mapping method for tobacco production line inspection robot based on improved RBPF to better meet the actual work needs. The wheel odometer and IMU data are fused using the extended Kalman filter algorithm, and the fusion odometer motion model and LiDAR observation model are used as the hybrid scheme distribution. In the mixed scheme distribution, the iterative nearest point method is used to find the sampled particles in the high probability region, and the matching score of the particle matching scan is taken as the adaptation value. Then, the Drosophila optimization strategy is used to adjust the particle distribution, and the weight of each optimized particle is solved. According to the weight of the solution, we adaptively do resampling. Finally, the detection map of the production line detection robot is updated according to the updated position and attitude information and the observation information of the tobacco production line detection robot particles.

II. LASER RADAR SLAM MAPPING OF TOBACCO PRODUCTION LINE INSPECTION ROBOT

A. Introduction to RBPF-SLAM Algorithm

In the problem of laser radar SLAM mapping of tobacco production line inspection robot, the theory of probability can be used to mitigate the impact of uncertain factors on the results [11]. Particle filter is not limited by linear Gaussian system, so it can be applied to any nonlinear non Gaussian dynamic system, and has reliable effect in target tracking and positioning [12]. The particle filter RBPF method is applied to the problem of laser radar SLAM mapping of tobacco production line patrol robots. The problem of laser radar SLAM mapping is decomposed into the problem of positioning of tobacco production line patrol robots and the problem of building environmental feature maps based on pose estimation, which can significantly reduce the computational complexity of laser radar SLAM mapping of tobacco production line patrol robots, and has super robustness. It is especially suitable for completing the laser radar SLAM mapping of the tobacco production line inspection robot in small and medium-sized scenes [13].

The core idea of the RBPF-SLAM algorithm is to describe the SLAM problem as a posterior probability of the trajectory in the form of probability [14]. In practical work, the RBPF-SLAM algorithm mainly uses the observation information of the laser radar sensor and the information of the wheel odometer to estimate the environment map m position and posture status of inspection robot in tobacco production line the joint posterior probability of $x_{1:t}$ [15] can be described as $p(x_{1:t}, m | z_{1:t}, u_{1:t-1})$, where, $z_{1:t}$ is marked with observation information obtained by LiDAR, including:

$$z_{1:t} = z_1, z_2, \dots, z_t \quad (1)$$

Among them, z_1 , z_2 as well as z_t refers to each element in the observation information sequence.

$u_{1:t-1}$ is marked with odometer information, including:

$$u_{1:t-1} = u_1, u_2, \dots, u_{t-1} \quad (2)$$

Among them, u_1 , u_2 as well as u_{t-1} are the elements in the odometer information sequence. The RBPF particle filter can be decomposed as follows by using Bayesian formula:

$$p(x_{1:t}, m | z_{1:t}, u_{1:t-1}) = p(m | x_{1:t}, z_{1:t}) p(x_{1:t} | z_{1:t}, u_{1:t-1}) \quad (3)$$

In formula (3), the environment map m trajectory of inspection robot for tobacco production line $x_{1:t}$ the joint posterior probability of is decomposed into the product of two independent posterior probabilities. The motion trajectory of the tobacco production line inspection robot is estimated first, and then the environment map is updated from the motion trajectory combined with the observation data. Among them,

$p(x_{1:t} | z_{1:t}, u_{1:t-1})$ is the posterior probability of the motion path, $p(m | x_{1:t}, z_{1:t})$ is a posteriori probability of the map. Particle filter is required to estimate the potential motion trajectory. At the same time, each particle has a motion trajectory. The final environment map is constructed from the movement tracks of these particles and the observation of the system.

The solution of $p(m | x_{1:t}, z_{1:t})$ is usually based on the extended Kalman filter algorithm, which uses occupancy grid mapping and reverse sensor model to generate planar grid maps, m is divided into a finite number of mesh elements m_i , where each cell contains a value that represents the probability of its being occupied $p(m_i)$, whose values range from "0" to "1". "0" means not occupied, and "1" means fully occupied. The posterior probability density of the map can be approximated as:

$$p(m | x_{1:t}, z_{1:t}) = \prod_i p(m_i | x_{1:t}, z_{1:t}) \quad (4)$$

Among them, i represents the number of particles.

$p(x_{1:t} | z_{1:t}, u_{1:t-1})$ using particle filter algorithm to solve it means that a particle will represent a potential trajectory in a time step and generate a map at the same time. According to Bayesian criteria to have the formula derivation of $p(x_{1:t} | z_{1:t}, u_{1:t-1})$:

$$p(x_{1:t} | z_{1:t}, u_{1:t-1}) = \eta p(z_t | x_t) p(x_t | x_{t-1}, u_t) p(x_{t-1} | z_{1:t-1}, u_{1:t-1}) \quad (5)$$

Among them, η is marked with normalization factor; $p(x_{1:t-1} | z_{1:t-1}, u_{1:t-1})$ represents the trajectory of the tobacco production line inspection robot at the previous time, represented by the particle swarm at the previous time; $p(x_t | x_{t-1}, u_t)$ indicates that the tobacco production line inspection robot is in the $t-1$ Position and posture at every moment x_{t-1} Tobacco production line inspection robot $t-1$ reach t time odometer data u_t when known, the tobacco production line inspection robot t time position and posture the probability distribution of x_t ; $p(z_t | x_t)$ represents the probability distribution of sensor observation data.

In actual work, the environment map of tobacco production line inspection robot is known m with the tobacco production line inspection robot t time position and posture x_t is available

$p(z_t | x_t, m)$ indicates sensor observation data of the probability distribution of z_t . Since many mobile robots are driven by independent translational and rotational speeds, the speed motion model is used for mileage distribution in this paper. After a series of derivation, the trajectory estimation of the tobacco production line inspection robot can be transformed into the corresponding incremental estimation problem. After obtaining the trajectory of the tobacco production line inspection robot, the map is constructed according to the estimated trajectory and observation data.

The RBPF-SLAM algorithm uses the sequential importance resampling filter to estimate the position and pose of the tobacco production line patrol robot and update the environment map. The specific process can be divided into the following four steps:

1) Sampling: as proposed distribution based on motion model $q(x_{1:t}^{(i)} | z_{1:t}, u_{1:t-1})$ sampling, $x_{1:t}^{(i)}$ is the pose of the particle. By particle set $\{x_{t-1}^{(i)}\}$ generate next generation particle sets $\{x_t^{(i)}\}$, where $i = 1, 2, \dots, N$, N is the total number of particles.

2) Weight solving. Resampling according to importance requires solving the weight of each particle $w_t^{(i)}$, the calculation formula is:

$$w_t^{(i)} = \frac{p(x_{1:t} | z_{1:t}, u_{1:t-1})}{q(x_{1:t}^{(i)} | z_{1:t}, u_{1:t-1})} \quad (6)$$

3) Resample. Resampling is performed according to the size of the solved importance weight to form a new particle set. The total number of particles remains unchanged, and each particle has the same weight after resampling N .

4) Map update. Pose of passing particles $x_{1:t}^{(i)}$ and observations $z_{1:t}$ to update the corresponding map $p(m^{(i)} | x_{1:t}^{(i)}, z_{1:t})$.

B. Improve the Laser Radar SLAM Mapping of RBPF Tobacco Production Line Inspection Robot

a) Information Fusion of Odometer and IMU: In this paper, EKF (Extended Kalman Filter) algorithm is used to estimate the position and pose information of mobile robots, and the state model of position and pose fusion is established using wheel odometer and IMU. Since the odometer and IMU data both contain the steering angle and speed information of the mobile robot, the pose state vector of the tobacco production line patrol robot can be described as:

$$x_t = (X_t, Y_t, \theta_t, v_x^t, v_y^t, \omega_t)^T \quad (7)$$

Among them, tobacco production line inspection robot of the position t , attitude and speed information of the time are respectively used (X_t, Y_t, θ_t) , (v'_x, v'_y, ω_t) to mark; T stands for transposition.

If the system status at the moment t is x_t , control input is $(v'_x, v'_y, \omega_t)^T$, and within a certain period of time Δt if it remains unchanged within a certain period of time, then after Δt , the tobacco production line inspection robot $t+1$ the position and posture at all times shall be x_{t+1} . Therefore, the EKF state transfer equation can be obtained as follows:

$$x_{t+1} = x_t + \begin{pmatrix} \Delta t & 0 & 0 \\ 0 & \Delta t & 0 \\ 0 & 0 & \Delta t \\ 0 & 0 & 0 \\ 0 & 0 & 0 \\ 0 & 0 & 0 \end{pmatrix} (v'_x, v'_y, \omega_t)^T \quad (8)$$

Since the odometer data can be obtained directly, the corresponding prediction equation can be obtained as follows:

$$z_{odom,t} = H_{odom} x_t = I_6 (X_t, Y_t, \theta_t, v'_x, v'_y, \omega_t)^T + e_{odom,t}(d) \quad (9)$$

Among them, the predicted value of wheel odometer $z_{odom,t}$ is marked; Prediction matrix of wheel odometer I_t use H_{odom} to mark; $e_{odom,t}(d)$ is the error of the wheel odometer, which obeys the covariance matrix of Gaussian distribution.

In this paper, we only study the environment map in two-dimensional space, so we only need the Z-axis data in the three-axis for IMU, so the prediction equation of IMU can be described as:

$$\begin{aligned} z_{IMU,t} &= H_{IMU,t} x_t \\ &= \begin{pmatrix} 0 & 0 & 1 & 0 & 0 & 0 \\ 0 & 0 & 0 & 0 & 0 & 1 \end{pmatrix} (X_t, Y_t, \theta_t, v'_x, v'_y, \omega_t)^T + e_{IMU,t} \\ &= \begin{pmatrix} \theta_t \\ \omega_t \end{pmatrix} + e_{IMU,t} \end{aligned} \quad (10)$$

Among them, $z_{IMU,t}$ IMU predicted value is marked; $H_{IMU,t}$ IMU prediction matrix is marked; $e_{IMU,t}$ IMU prediction error is marked, which obeys Gaussian distribution covariance matrix.

The prediction equation of the system can be obtained by combining the prediction equation of the wheel odometer and IMU, which can be described as:

$$z_t = \begin{pmatrix} z_{odom,t} \\ z_{IMU,t} \end{pmatrix} = \begin{pmatrix} H_{odom,t} \\ z_{IMU,t} \end{pmatrix} x_t + \begin{pmatrix} e_{odom,t}(d) \\ e_{IMU,t} \end{pmatrix} \quad (11)$$

By substituting the state transition equation and prediction equation of the position and posture information of the tobacco production line patrol robot into the Kalman filter formula, the position and posture of the tobacco production line patrol robot can be accurately estimated.

b) Distribution of Improvement Proposals: In general, the target distribution is more difficult to obtain an analytical solution than the proposed distribution. Therefore, in practical work, the proposed distribution is often introduced and sampled to approximate the target distribution according to the weight of particles and resampling [16]. The closer the proposed distribution is to the target distribution, the better the effect of particle filter will be [17]. In the RBPF-SLAM algorithm described above, the motion model of the inspection robot in the tobacco production line is regarded as the proposed distribution, and the particle weight is calculated according to the observation model of the inspection robot in the tobacco production line. This method of sampling from the motion model of the inspection robot in the tobacco production line, although relatively simple in calculation, is not accurate. Since the tobacco production line inspection robot will be equipped with a laser radar and a odometer, and the observation accuracy of the laser radar is far higher than the odometer accuracy, as shown in Fig. 1, the probability distribution density function of the odometer model has a wide span and is low and flat, while the probability distribution density function of the laser radar observation model has a small span and is high and sharp. If only the odometer model is used for sampling, a large number of particles will be in meaningless areas. After resampling, these meaningless particles will be discarded. There are fewer particle types in meaningful areas, making the effect of particle filtering worse.

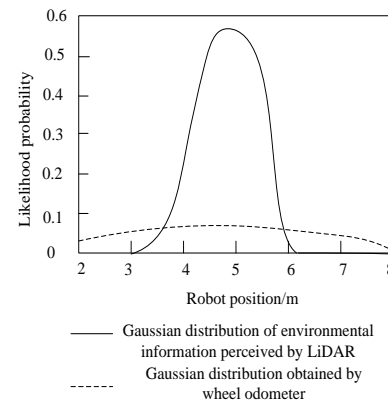


Fig. 1. Legend of distribution density function for LiDAR and odometer measurement models

For this reason, the LiDAR observation value is considered when sampling particles z_t to improve the proposal distribution, and describe the improved proposal distribution as:

$$\Gamma(x_t) = p(z_t | x_t, m^{(i)}) p(x_t | x_{t-1}^{(i)}, u_t) \quad (12)$$

Among them, $\Gamma(x_t)$ is marked the proposed distribution after improvement; $x_{t-1}^{(i)}$ marks the first generation of the previous generation i particles; $m^{(i)}$ is according to the previous generation i current environment map estimated by particles; u_t is according to the previous generation i current odometer information estimated by particles.

After improvement, the proposed distribution comprehensively considers odometer information and LiDAR observation information, and concentrates particles in the high probability interval, which improves the quality of particle set.

c) *Laser Information Scanning Matching*: Considering the characteristics of laser radar scanning, this paper introduces the scanning matching method to calculate the transformation between adjacent laser frames. Scanning matching is to compare two different laser frame information and register them. In other words, it is to find a suitable rotation and translation method, which corresponds the points between different laser frames one by one to get the rotation and translation information of the inspection robot in the tobacco production line. Here, the estimated information of particles is used to register with the laser information, and the analytical formula of the LiDAR distribution is obtained to avoid the error caused by the EKF linearization method.

At present, the commonly used and effective scanning matching method is the iterative closest point method (ICP) [18]. Its principle is the optimal matching based on the least square method, and its main contents include: determining the corresponding relationship of each point cloud data; Calculating transformation matrix; Find the minimum error until the error reaches the set threshold. The specific solution steps are as follows:

1) First, suppose that the laser radar carried by the tobacco production line inspection robot is t the laser data and particle prediction data scanned at any time are L, C , and has:

$$L = \{l_1, l_2, \dots, l_n\} \quad (13)$$

$$C = \{c_1, c_2, \dots, c_n\} \quad (14)$$

Among them, l_1, l_2 as well as l_n are points in the laser data, n marked is the number of points; c_1, c_2 as well as c_n marked are the points in the particle prediction data.

In actual work L as t template point set at time, C as t the set of punctual points to be allocated at the time. About C and L select the point with the smallest Euclidean distance as the corresponding point, and add it to the temporary matching point set.

2) Decentralize each point set to solve L, C and mark their centroids as u_L, u_C , then remove u_L, u_C from L, C .

3) After knowing the corresponding relationship of each point set, solve the objective function shown in equation (15).

$$E(R, T) = \frac{1}{n_C} \sum_{i=1}^{n_C} \|l_i - Rc_i - T\|^2 \quad (15)$$

Among them, $E(R, T)$ the scanning matching error function is marked; For the rotation matrix of point set R to mark; The translation matrix of the point set is used T to mark; l_i, c_i is the corresponding point in the temporary corresponding point set; n_C is marked the number of data points in the particle prediction data set at the current time.

The process of solving the inter frame registration is the process of solving the minimum value of the objective function shown in equation (15), which is completed by using the singular value decomposition method in this paper.

a) *Adaptive Resampling*: Since the RBPF-SLAM algorithm only uses the motion model as the proposed distribution, as time goes on, the cumulative error of the odometer becomes larger and larger, which reduces its estimation performance [19]. For this reason, corresponding improvements have been made in the above sections. When using the motion model to calculate the proposed distribution, the optical observation information has been added, so as to obtain a better proposed distribution. Since the resampling step also has an important impact on particle filtering, during resampling, particles with high weight are usually replaced by particles with low weight. However, frequent resampling operations may eliminate effective particles and cause particle degradation. Therefore, the resampling step is improved adaptively, and a variable to measure particle degradation severity is proposed N_{eff} , which can be described as:

$$N_{eff} = \frac{1}{\sum_{i=1}^N (\tilde{\omega}^{(i)})^2} \quad (16)$$

Wherein, i the weight of particles is marked as $\tilde{\omega}^{(i)}$; For effective particle number is marked as N_{eff} .

In actual work, usually the smaller the value of N_{eff} is, the more serious the particle degradation is. The larger the value is, the better the diversity of particles is. Usually when the N_{eff}

descend to $0.5N$, the resample is performed, and each particle will get the same weight after resampling. Adaptive resampling can resample when the system needs, reduce the number of resampling, and improve the robustness of the algorithm.

b) Drosophila Optimization Strategy: In view of the advantages of the Fruit Fly Optimization Algorithm (FOA) algorithm in target optimization [20], this paper introduces it into the laser radar SLAM mapping work of the tobacco production line inspection robot, and effectively integrates the FOA algorithm and RBPF algorithm to achieve more ideal SLAM mapping work effect.

The basic idea of the fusion is: after the sampling process is optimized and the proposed distribution of sampling particles is obtained, the particle set is regarded as the drosophila population, and the scan matching score is taken as the individual fitness value, which reflects the compliance of the individual with the real state of the tobacco production line inspection robot. The FOA algorithm is used to optimize the particle distribution, drive the drosophila individual to fly to the optimal position, and constantly search the surrounding area for a better position at random, so that the drosophila is constantly approaching the real state of the mobile tobacco production line inspection robot, and alleviate particle degradation.

The standard FOA algorithm regards each drosophila individual as a feasible solution, and constantly moves to the optimal position to seek the global optimal solution of the model. The process of FOA algorithm is as follows:

1) Initialization. Set parameters such as initial position, population size, maximum iteration number Maxgen of *Drosophila melanogaster*.

2) *Drosophila* flies out of the current position and randomly searches for higher concentration positions around. The movement formula is as follows:

$$x_k^{(i)} = x_{k-1}^{(i)} + RandValue \quad (17)$$

Among them, $x_{k-1}^{(i)}$ indicates the particle state at the last iteration; $x_k^{(i)}$ indicates the state of particles at the current time; *RandValue* indicates the step size of random movement.

3) The individual fitness value was obtained from the location concentration of *drosophila melanogaster*, and the optimal individual of the population was found.

4) If the current optimal fitness value is greater than the maximum fitness value of the previous iteration, all *drosophila* flies to the optimal individual. Repeat steps (2) to (4) until the termination conditions are met.

The number of particles determines the number of particles used to represent the state space in the RBPF algorithm. Increasing the number of particles can improve the accuracy and robustness of the algorithm, but at the same time increase the computational complexity. The algorithm usually requires

several iterations to converge to accurate location estimation and map building results. Increasing the number of iterations can improve the stability and accuracy of the results, but it also increases the computation time.

In order to overcome the limitation of the standard FOA algorithm in the convergence process that the population diversity decreases and the particles tend to fall into the local optimum, which leads to the deviation from the real state, this paper introduces the cross mutation operation to improve the adaptability of the population. After the particles are randomly paired, the cross operation is carried out according to the adaptive probability, and then a certain number of optimal particles are copied and mutated to maintain the diversity of the population, prevent falling into local optimal solution. Finally, the state update formula of exponential function step size is used to move *drosophila* individuals to increase the optimization step size, improve the convergence speed of the algorithm, and help the algorithm jump out of the local optimum.

The improved individual renewal formula of *drosophila melanogaster* is:

$$x_k^{(i)} = x_{k-1}^{(i)} + e^{rand} - 1 \quad (18)$$

Among them, e^{rand} represents the step size of exponential function.

By introducing the improved FOA algorithm, the estimation accuracy of the filter can be effectively improved and improved, so that the number of particles required is reduced, thus reducing the calculation amount of the algorithm, and effectively solving the problems of insufficient population diversity and poor real-time performance when completing the laser radar SLAM mapping of the tobacco production line inspection robot based on RBPF.

a) RBPF-SLAM Algorithm Improvement Process

1) The precise motion model and laser radar joint model obtained by fusing the wheel odometer and IMU data are distributed as improvement proposals at the moment $t=0$, select particles N and the weight of particles is N .

2) In the hybrid proposed distribution, the iterative closest point method is used to scan and match to find out the sampling particles in the high probability area, sample in the matched particle set, and take the matching score of the particle matching scan as the fitness value f_i , adjust the particle distribution using the *drosophila* optimization strategy.

3) Calculate, update and normalize the weight of optimized particles, if N_{eff} descend to $0.5N$ start the resample operation.

4) The map is updated according to the position and posture information and observation information of the tobacco production line inspection robot. The improved RBPF-SLAM algorithm flow is shown in Fig. 2.

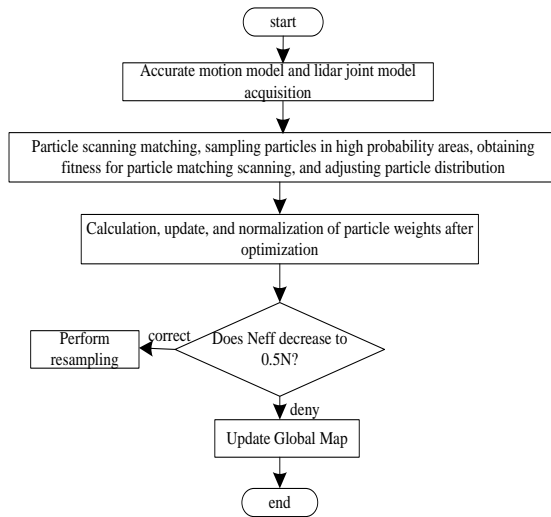


Fig. 2. Improved RBPF-SLAM algorithm process.

III. EXPERIMENT AND ANALYSIS

As an important part of the daily production and management of tobacco production companies, whether the inspection robot of tobacco production line can better realize the laser radar SLAM mapping is directly related to whether the daily inspection task of tobacco production line can be effectively completed. Therefore, in this experiment, the inspection robot of a large tobacco company's production line is taken as the experimental object. The method in this paper is applied to its SLAM mapping, and the effectiveness of the method in this paper is verified. It is reported that the tobacco company was established in June 1984, and two tobacco distribution companies were established in October of the same year. By December 2016, in addition to the original two tobacco distribution companies, it was found that there was a large demand for tobacco marketing in this area, so five tobacco production companies were established in succession. After the establishment of tobacco production companies, it was found that the traditional manual inspection mode was no longer suitable for the long-term development needs of tobacco companies. Therefore, a large number of inspection robots for tobacco production lines were introduced into the newly established five tobacco production branches to assist the production of tobacco production companies and help the development of tobacco enterprises. The introduced tobacco production line inspection robots and their technical parameters are shown in Fig. 3 and Table I. The chassis of the tobacco production line inspection robot uses two wheels for differential movement, and is loaded with wheel odometer, IMU and two-dimensional laser radar. In this experiment, the two groups of tobacco production line patrol robots built in this experiment are respectively 18m * 15m and 24m * 23m in size. In addition, the tobacco production line patrol robots also have a 3D visualization tool RVIZ, which is used to display the laser radar point cloud in the experiment and draw the environment map in real time.

The two-dimensional grid map constructed with 15 sampling particles using the method in this paper is shown in Fig. 4. Among them, the white area is the area that has been scanned by the laser radar, the black line represents the outline

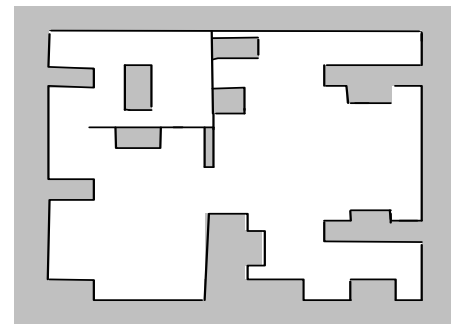
of the object, and the gray area is the map area that has not been scanned by the laser radar.



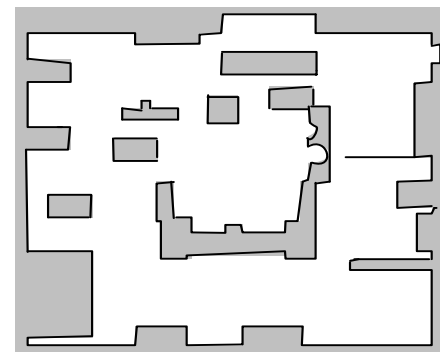
Fig. 3. Tobacco production line inspection robot.

TABLE I. MAIN TECHNICAL PARAMETERS OF TOBACCO PRODUCTION LINE INSPECTION ROBOTS

Parameter information	Parameter value
Model	M-20iA
Overall weight	40kg
Dimensions	800*450*200mm
Gradeability	30°
Fastest running speed	1m/s
Turning radius	2000mm
Visual resolution	1080P
Inspection efficiency	10s/inspection point
Navigation method	Laser SLAM
Repeatability	±10mm



(a) 18m*15m



(b) 24m*23m

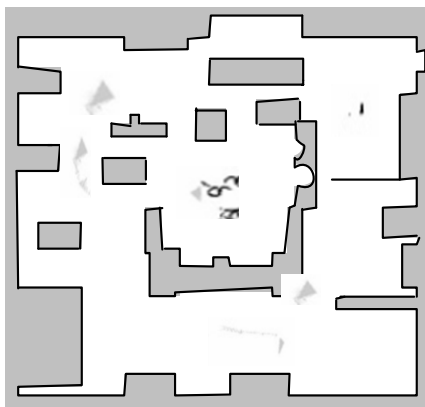
Fig. 4. The method used in this article to construct an environmental map.

It can be seen from Fig. 4 that the method in this paper can realize the laser radar SLAM mapping of the tobacco production line inspection robot, and the environment map constructed is relatively clear, which can better meet the actual work needs. This is mainly because the improved FOA algorithm introduced in the proposed method can effectively improve and increase the estimation accuracy of the filter, thus reducing the number of particles required, thus reducing the calculation amount of the algorithm, and effectively solving the problem of insufficient population diversity and poor real-time performance when the tobacco production line inspection robot based on RBPF completes the LiDAR SLAM mapping.

Fig. 5 is a two-dimensional grid map constructed by the traditional RBPF-SLAM method using 30 sampling particles.



(a) 18m*15m



(b) 24m*23m

Fig. 5. Traditional RBPF-SLAM method for constructing environmental maps.

It can be seen from Fig. 5 that the two-dimensional grid map constructed by the traditional RBPF-SLAM method has a large error, and there are deviations in many parts, such as incomplete scanning in the white area. Compared with the two-dimensional grid map constructed by using 15 sampling particles in Fig. 4, the effect is obviously worse, which is undoubtedly another verification of the effectiveness of this method. This is mainly because the method proposed in this paper uses the exponential function step length state update formula to move fruit flies, increase the optimization step size,

improve the convergence speed of the algorithm, and make the algorithm jump out of the local optimal solution.

In order to further verify the effectiveness of the method in this paper, within 200s, the method in this paper will be reasonably compared with the traditional RBPF-SLAM method in the laser radar SLAM mapping of the tobacco production line inspection robot, and the obtained position and attitude state error comparison curve is shown in Fig. 6.

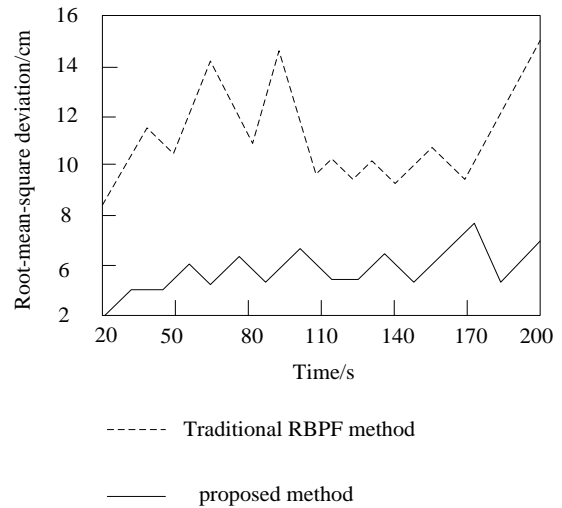
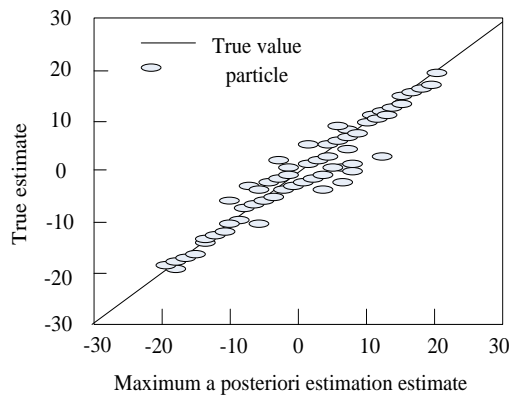


Fig. 6. Comparison curve of pose state error.

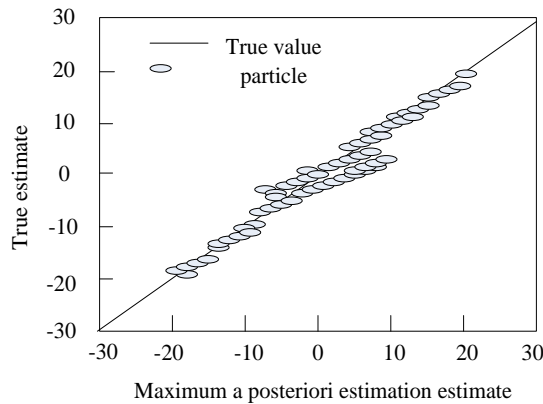
It can be seen from the pose state estimation curve of the tobacco production line patrol robot shown in Fig. 6 that the position state estimation error of the tobacco production line patrol robot obtained by applying the method in this paper to implement laser radar SLAM mapping of the tobacco production line patrol robot is significantly lower than the traditional RBPF-SLAM method. This is mainly because when the method in this paper is used to estimate the position and orientation of the tobacco production line patrol robot, the wheel odometer information and IMU information of the tobacco production line patrol robot are effectively fused, so the position and orientation estimation accuracy of the tobacco production line patrol robot is higher.

Fig. 7 shows the particle distribution after particle filtering of this method and the traditional RBPF-SLAM method.

It can be seen from Fig. 7 that the fitting accuracy of the filtering method in this paper is higher. After filtering, most particles are closely distributed and close to the true value, and there is almost no divergence of particle samples. After traditional RBPF-SLAM filtering, the distribution of particles is relatively divergent, and some particles are far from the true value. Note: The method in this paper has more advantages in the accuracy of map estimation, and can better meet the needs of the actual tobacco production line inspection robot laser radar SLAM mapping work. This improved filtering method has a great advantage in map estimation accuracy, and can well meet the needs of the actual tobacco production line inspection robot LiDAR SLAM mapping.



(a) Particle distribution after filtering using traditional RBPF-SLAM method



(b) Particle distribution after filtering in this method

Fig. 7. Comparison of particle distribution after filtering.

IV. CONCLUSION

The method in this paper can realize the laser radar SLAM mapping of tobacco production line patrol robot, and the mapping effect is good. Its advantages in the laser radar SLAM mapping of tobacco production line patrol robot mainly include:

1) Compared with the traditional RBPF-SLAM method, the method in this paper can build an ideal inspection map of the tobacco production line inspection robot with fewer particles, and the two-dimensional grid map constructed is clearer, which can better meet the actual work needs.

2) Compared with the traditional RBPF-SLAM method, the method in this paper is used to implement the laser radar SLAM mapping for the tobacco production line patrol robot, which can obtain lower position and attitude state estimation error of the tobacco production line patrol robot, and has better fitting accuracy when filtering. After filtering, most particles are closely distributed and close to the true value, and there is almost no divergence of particle samples.

3) The wheel odometer and IMU data are fused using the extended Kalman filter algorithm, and the fusion odometer motion model and LiDAR observation model are adopted as the hybrid scheme distribution. In the mixed scheme distribution, the iterative nearest point method is used to find the sampled particles in the high probability region, and the

matching score of the particle matching scan is taken as the adaptation value.

4) RBPF needs to process a large number of particles to represent the state space, and perform state estimation and map update, which leads to high computational complexity, especially in real-time applications may face the problem of processing time delay. Future research could explore more efficient algorithms, such as improved versions of RBPF based on reducing the number of particles or introducing other optimization methods.

REFERENCES

- [1] Cattaneo, D. , Vaghi, M. , & Valada, A. (2022). Lcdnet: deep loop closure detection and point cloud registration for lidar slam. *IEEE Transactions on Robotics: A publication of the IEEE Robotics and Automation Society*, 38(4), 2074-2093.
- [2] Chunrong, Z. (2021) Bending limit test of robot arm material[J], *Ordance Material Science and Engineering*, 44(4), 120-124.
- [3] Peichao, C. , Kunfeng, L. , & Jiachao, Z. (2023) SLAM and Path Planning for Mobile Robots in Complex Scenes[J], *Computer simulation*, 40(2), 443-448,458.
- [4] Kudriashov, A. , Buratowski, T. , Garus, J. , & Giergiel, M. (2021). 3d environment exploration with slam for autonomous mobile robot control. *WSEAS Transactions on Systems and Control*, 16, 450-456.
- [5] Koval, A. , Karlsson, S. , & Nikolakopoulos, G. (2022). Experimental evaluation of autonomous map-based spot navigation in confined environments. *Biomimetic Intelligence and Robotics*, 2(1), 50-58.
- [6] Park, C. , Moghadam, P. , Williams, J. L. , Kim, S. , Sridharan, S. , & Fookes, C. (2022). Elasticity meets continuous-time: map-centric dense 3d lidar slam. *IEEE Transactions on Robotics: A publication of the IEEE Robotics and Automation Society*, 38(2), 978-997.
- [7] Michal Mihálik, Malobick, B. , Peniak, P. , & Vesteňick, P. (2022). The new method of active slam for mapping using lidar. *Electronics*, 11(7), 1082.
- [8] Karimi, M. , Oelsch, M. , Stengel, O. , Babaian, E. , & Steinbach, E. (2021). Lola-slam: low-latency lidar slam using continuous scan slicing. *IEEE Robotics and Automation Letters*, PP(99), 1-1.
- [9] Bol, N. , Duramaz, M. , Ztrk, E. , Durdu, A. , & Yildiz, B. (2021). Convolutional neural networks based active slam and exploration. *European Journal of Science and Technology*(22), 342-346.
- [10] Gerlein, E. A. , Gabriel Díaz-Guevara, Carrillo, H. , Parra, C. , & Gonzalez, E. (2021). Embedded system-on-chip 3d localization and mapping—esoc-slam. *Electronics*, 10(12), 1378.
- [11] Miller, I. , Cowley, A. , Konkimalla, R. , Skandan, S. , & Kumar, V. (2021). Any way you look at it: semantic crossview localization and mapping with lidar. *IEEE Robotics and Automation Letters*, PP(99), 1-1.
- [12] Sugiura, K. , & Matsutani, H. (2021). A universal lidar slam accelerator system on low-cost fpga, 10(Mar.8), 26931-26947.
- [13] Park, Y. S. , Shin, Y. S. , Kim, J. , & Kim, A. (2021). 3d ego-motion estimation using low-cost mmwave radars via radar velocity factor for pose-graph slam. *IEEE Robotics and Automation Letters*, PP(99), 1-1.
- [14] Lowe, T. , Moghadam, P. , Edwards, E. , & Williams, J. (2021). Canopy density estimation in perennial horticulture crops using 3d spinning lidar slam. *Journal of Field Robotics*, 38(4), 598-618.
- [15] Kim, H. , & Choi, Y. (2021). Location estimation of autonomous driving robot and 3d tunnel mapping in underground mines using pattern matched lidar sequential images. *Journal of Mining Science and Technology: English Edition*, 031(005), 779-788.
- [16] Sung, C. , Jeon, S. , Lim, H. , & Myung, H. (2022). What if there was no revisit? large-scale graph-based slam with traffic sign detection in an hd map using lidar inertial odometry. *Intelligent Service Robotics*, 15(2), 161-170.
- [17] Trybala, P. , John, A. , & Kohler, C. (2022). Towards a mine 3d dense mapping mobile robot: a system design and preliminary accuracy evaluation. *Markscheidewesen*, 129(1) , 18-24.

- [18] Ali, W. , Sheng, L. , & Ahmed, W. (2021). Robot operating system-based slam for a gazebo-simulated turtlebot2 in 2d indoor environment with cartographer algorithm, 15(3), 149-157.
- [19] Belkin, I. , Abramenko, A. , & Yudin, D. (2021). Real-time lidar-based localization of mobile ground robot. *Procedia Computer Science*, 186(14), 440-448.
- [20] Funabiki, N., Morrell, B. , Nash, J. , & Agha-Mohammadi, A. A. (2021). Range-aided pose-graph-based slam: applications of deployable ranging beacons for unknown environment exploration. *IEEE Robotics and Automation Letters*, 6(1), 48-55.